JOURNAL OF ELECTROMAGNETIC ENGINEERING AND SCIENCE, VOL. 24, NO. 3, 234~242, MAY. 2024

https://doi.org/10.26866/jees.2024.3.r.224
ISSN 2671-7263 (Online) · ISSN 2671-7255 (Print)

Design of a Compact Log Periodic Dipole Array Antenna for Broadband and High-Power Beam Synthesis Using Superposition

Changhyeon Im[1] · Sangwoon Youn[1] · Tae Heung Lim[2] · Hosung Choo[1,*]

Abstract

This paper investigates various array beam shapes for high-power electronic warfare applications using an actual broadband array antenna. For use in a limited mounting space, a compact printed log periodic dipole array (LPDA) operating over a wide bandwidth is designed. The LPDA is then extended to an 8 × 1 array, with active element patterns (AEPs) obtained through simulation and measurement. Beam synthesis is performed by the superposition of several array patterns, which involves adjusting the weight of each AEP. To derive a synthesized array beam shape that is similar to the guided mask, the Taylor window weighting method is applied to each array pattern. Finally, beam synthesis for the flat-top beam, cosecant-squared beam, and iso-flux beam is performed using Taylor window-weighted AEPs, and the results are compared with those of beam shapes using ideal isotropic patterns. The results demonstrate that various beam shapes can be achieved for high-power electronic warfare applications using the AEPs of an actual array antenna.

Key Words: Active Element Patterns (AEPs), Beam Synthesis, Broadband, Log Periodic Dipole Array (LPDA).

I. Introduction

In the field of electronic warfare, the use of various array antenna systems capable of beamforming over a wide bandwidth using high-power radiation has been gradually increasing [1–3]. Such systems are often necessary in critical electronic warfare systems, such as high-power jammers, long-range radars, and target direction-finding systems, which play key roles in establishing a superior electromagnetic spectrum environment [4–6]. For example, broadband jammers used in avionics warfare typically operate within the frequency range of 1–18 GHz, while long-range radars used in ground stations function within the 2–4 GHz range [7]. Furthermore, direction-finding systems for detecting unauthorized transmitters often operate in the 1–40 GHz range. Since these high-power broadband systems are usually mounted on an aircraft, vehicle, or ground base station, which offers limited mounting space, a small-sized array antenna that satisfies wide bandwidth operations is required. Various types of broadband antennas, such as a ridged horn, an antipodal Vivaldi, and a log periodic dipole array (LPDA), have been extensively studied for use in these systems [8, 9]. Furthermore, in terms of power efficiency, an array antenna system that can form various shapes of beam patterns by adjusting the magnitude and phase of individual antenna elements is crucial [5, 10–15].

Manuscript received April 12, 2023 ; Revised July 15, 2023 ; Accepted September 22, 2023. (ID No. 20230412-073J)
[1]Department of Electronic and Electrical Engineering, Hongik University, Seoul, Korea.
[2]School of Electronic Engineering, Kumoh National Institute of Technology, Gumi, Korea.
[*]Corresponding Author: Hosung Choo (e-mail: hschoo@hongik.ac.kr)

Therefore, beam synthesis studies have been conducted primarily for wireless communication and wireless power transmission applications [16, 17]. Recently, it has been applied to specific electronic warfare situations. For example, a flat-top beam can be used to uniformly transmit signals to a number of systems, cosecant-squared beams can be employed for air-to-ground scanning, and an iso-flux beam can be used at high altitudes to transmit uniform power to the ground. However, most studies have yielded only theoretical beam synthesis results, assuming that the array elements are ideal isotropic sources. In actual array antennas, each antenna element has different radiation patterns with mutual couplings. As a result, unexpected performance degradations, such as phase changes in antenna ports, reduction of radiation gain, and distortion in the radiation pattern, are observed in many cases. These problems also lead to distorted or unintended results pertaining to synthesized array beam shapes. Therefore, it is necessary to identify and study methods that can help obtain various beam shapes for specific purposes by accounting for the different radiation patterns and mutual couplings of each array element.

In this paper, various array beam shapes for high-power electronic warfare applications are derived using an actual broadband array antenna. For high-power arrays to be applied in a limited mounting space, a compact printed LPDA operating over a wide bandwidth is designed. To confirm the broadband characteristics of the designed antenna, the LPDA is fabricated, and its antenna performances, such as reflection coefficients and radiation patterns, are measured in a full anechoic chamber. The LPDA is then extended to an 8 × 1 array, and the active element patterns (AEPs) of the individual elements, considering their mutual couplings, are obtained by conducting measurements as well as simulations. Following this, after adjusting the weights of each AEP, beam synthesis within the guided mask is performed by the superposition of several array patterns with different steering angles and amplitudes. To derive synthesized array beam shapes that closely resemble the guided mask, the Taylor window weighting method is applied to each array pattern. Finally, beam synthesis for a flat-top beam, a cosecant-squared beam, and an iso-flux beam is performed using the Taylor window-weighted AEPs. The results are then compared with those of the beam shapes using ideal isotropic patterns, ultimately demonstrating that various beam shapes for high-power electronic warfare, such as the flat-top beam, the cosecant-squared beam, and the iso-flux beam, can be achieved using the AEPs of the actual array antenna.

II. Design and Measurement of the Broadband LPDA and its Array

1. Broadband LDPA

Fig. 1 presents the geometry of the proposed compact LPDA for high-power broadband beamforming applications. The LPDA element was optimized to satisfy broadband characteristics operating within the 2–5 GHz range and boresight gain of more than 3 dBi for high-power beamforming systems, which typically allow limited antenna mounting space. The optimized antenna was printed on an FR-4 substrate (ε_r = 4.3, tanδ = 0.018) to minimize the dimensions of length l_s, width w_s, and thickness t_s, as shown in Fig. 1(a)–1(c). In the LPDA design, a total of 13 dipole elements were employed to realize high directivity and broadband characteristics, which would help attain the various beam shapes required in electronic warfare systems. Each dipole element was designed considering a geometric ratio τ and an apex angle α, as expressed using equations as follows:

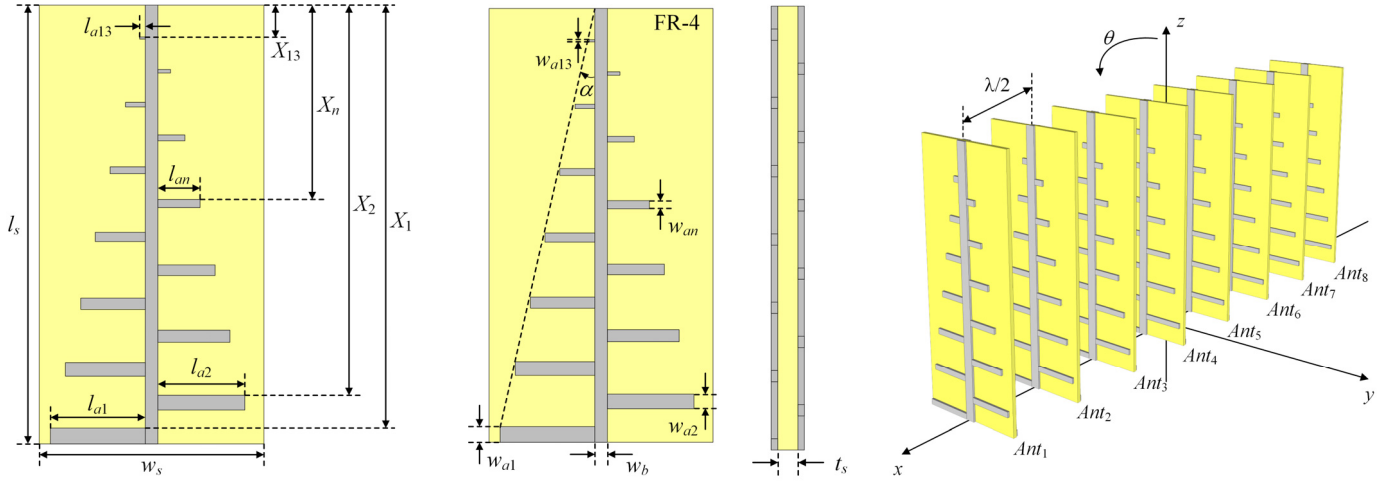

Fig. 1. Geometry of the proposed antenna: (a) top view, (b) bottom view, (c) side view, and (d) isometric view of the array antenna.

$$\tau = \frac{l_{a(n+1)}}{l_{an}} = \frac{X_{n+1}}{X_n}, \quad (1)$$

$$\alpha = \tan^{-1}\left(\frac{l_{an}}{X_n}\right). \quad (2)$$

As shown in Fig. 1(a) and 1(b), the geometric parameters of length l_{a1} and width w_{a1} of the longest element determined the lowest operating frequency to be 2 GHz. Subsequently, the other elements were sequentially designed with regard to the geometric ratio τ. Notably, l_{an} refers to the length of the n^{th} dipole element, while the length of the $(n+1)^{\text{th}}$ element can be given by $\tau \cdot l_{an}$. The position parameter X_n was then calculated in the same way. Meanwhile, the length l_{a13} and width w_{a13} at position X_{13} were designed to cover the highest operating frequency of 5 GHz. Furthermore, the relation between the length l_{an} and location X_n of the dipoles was determined by the apex angle α in Fig. 1(b). The boom located at the center of the substrate was designed to feed the dipole elements with a width of w_b and length of l_s. Notably, the dimensions of an LPDA, as determined by the two design factors (τ and α), have a significant impact on broadband impedance-matching characteristics. The optimized design parameters, the detailed values of which are listed in Table 1, were obtained using the CST Studio Suite EM simulation software (http://www.cst.com). The single LPDA element was then extended to an 8 × 1 linear array configuration, maintaining array spacing of λ/2 at 4 GHz to synthesize various beams for electronic warfare purposes, as shown in Fig. 1(d). It is quite obvious that array antennas equipped with a large number of elements have an advantage in beam synthesis due to the narrow half-power beam width (HPBW) of the array pattern [18–21]. However, there are some disadvantages as well—the array system should be bulky and heavy. To compensate for these disadvantages, this study derived the beam synthesis performance using only eight elements of the LPDA that exhibited high gain and broadband characteristics.

Fig. 2(a) presents a photograph of the fabricated single LPDA, which shows that the proposed antenna is directly fed by an SMA connector at the top of the boom. Fig. 2(b) illustrates the extended 8 × 1 array in the *x*-axis, along with the proposed LPDA. The eight array elements were fixed at exact positions by a multi-layered, lightweight Styrofoam jig. Fig. 3 presents the reflection coefficients with regard to the LPDA boom width w_b. It is observed that when w_b is 4 mm, the reflection is less than −10 dB in the 1.7–5 GHz range.

Table 1. Design parameters of the proposed antenna

Parameter	Value	Parameter	Value
l_s	124 mm	w_b	4 mm
w_s	72 mm	t_s	1.6 mm
l_{a1}	29 mm	w_{a1}	6 mm
l_{a2}	23.73 mm	w_{a2}	4.98 mm
l_{a3}	19.36 mm	w_{a3}	4.13 mm
l_{a4}	15.73 mm	w_{a4}	3.43 mm
l_{a5}	12.71 mm	w_{a5}	2.85 mm
l_{a6}	10.21 mm	w_{a6}	2.36 mm
l_{a7}	8.14 mm	w_{a7}	1.96 mm
l_{a8}	6.41 mm	w_{a8}	1.63 mm
l_{a9}	4.98 mm	w_{a9}	1.35 mm
l_{a10}	3.80 mm	w_{a10}	1.12 mm
l_{a11}	2.81 mm	w_{a11}	0.93 mm
l_{a12}	1.99 mm	w_{a12}	0.77 mm
l_{a13}	1.31 mm	w_{a13}	0.64 mm
X_1	118 mm	X_8	29.83 mm
X_2	97.43 mm	X_9	24.25 mm
X_3	80.36 mm	X_{10}	19.62 mm
X_4	66.19 mm	X_{11}	15.77 mm
X_5	54.42 mm	X_{12}	12.58 mm
X_6	44.66 mm	X_{13}	9.93 mm
X_7	36.56 mm	τ	0.83
α	0.25 rad	–	–

2. LDPA Array

Fig. 4 presents the measured and simulated active reflection coefficients (ARCs) of Ant_5 (the center element) of the proposed compact printed LPDA array. The measured ARCs show broadband characteristics of less than −10 dB within the 2.2–5 GHz range (fractional bandwidth of 93.3%), which agrees well with the simulation results. Furthermore, although a slight change in the reflection coefficient was observed due to mutual coupling changes when using the array antenna for the various beam synthesis estimations, no significant change could be identified. Therefore, the designed LPDA can be employed for high-power beamforming in electronic warfare systems with a wide bandwidth. Fig. 5 shows the results of mutual coupling between Ant_5 and the other elements. Furthermore, mutual couplings with Ant_1, Ant_2, Ant_3, and Ant_4 were measured. Notably, the mutual coupling with Ant_4 (the nearest element) was less than −10 dB between 1 GHz and 5 GHz. Fig. 6 presents the measured and simulated boresight gains of the 8 × 1 array antenna. The solid line indicates the simulation results, while the "×" markers represent the measurement results. It is observed that the measured boresight gains are more than 10 dBi from 2 GHz, with the simulation results showing a similar tendency. Fig. 7(a)–7(f) present the measured and simulated 2D AEPs of Ant_2 and Ant_5 at 2.5

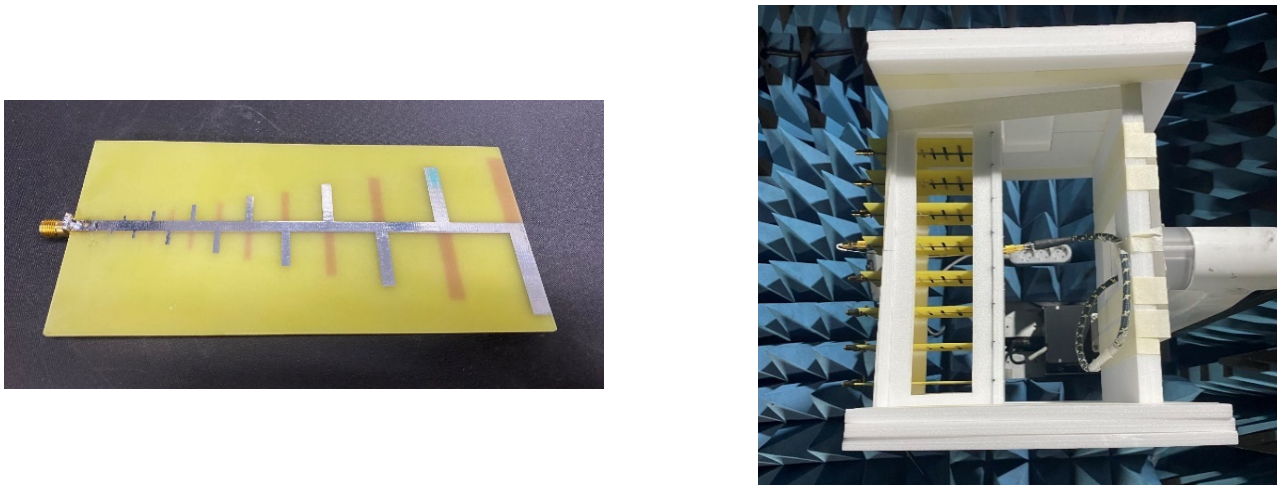

(a) (b)

Fig. 2. Photographs of the fabricated antenna: (a) single LPDA element and (b) 8 × 1 array configuration.

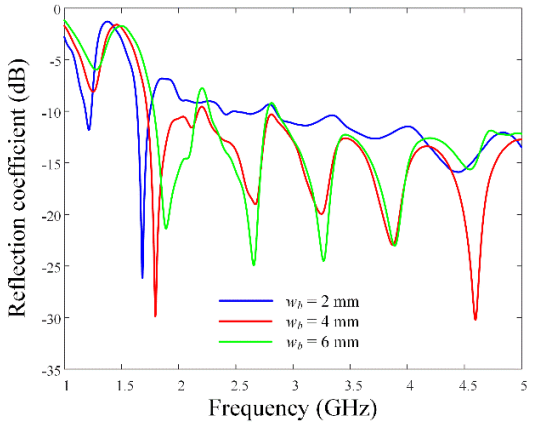

Fig. 3. Reflection coefficients in accordance with parameter w_b.

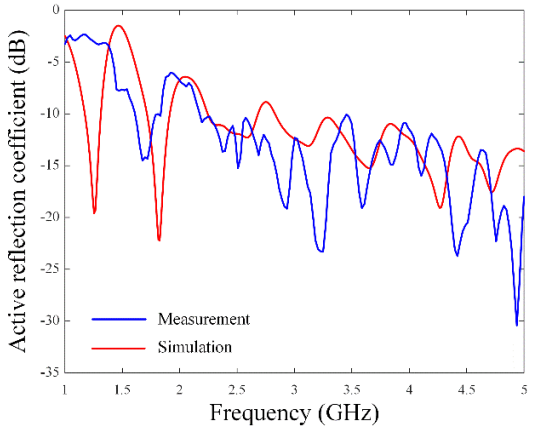

Fig. 4. Measured and simulated ARCs of the Ant_5 element.

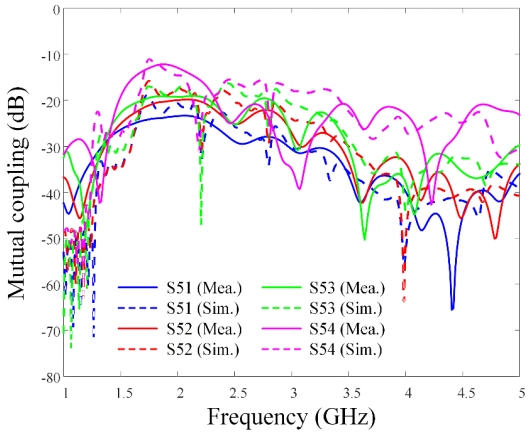

Fig. 5. Measured and simulated mutual couplings of the array antenna elements with Ant_5.

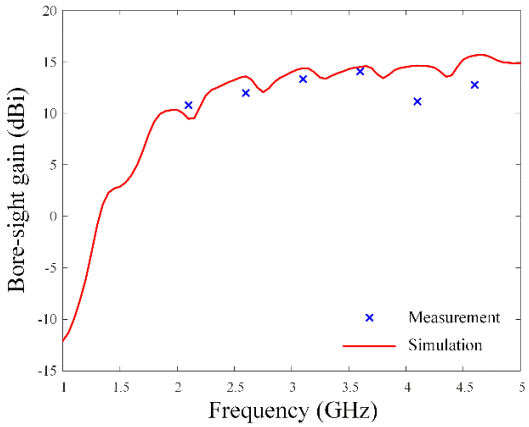

Fig. 6. Measured and simulated boresight gains of the array antenna according to frequency.

GHz, 3.5 GHz, and 4.5 GHz, respectively. As expected, Ant_2, which is located near the edge, has an asymmetric radiation pattern, while Ant_5, located at the center, has a symmetrical beam pattern. At 4.5 GHz, Ant_2 has a maximum gain of 6.3 dBi ($\theta = -56°$), and Ant_5 shows 6.0 dBi ($\theta = -22°$). However, since significant distortion is often observed in the patterns of individual elements in actual array antennas, it is necessary to use AEP instead of the ideal isotropic radiation pattern for beam synthesis.

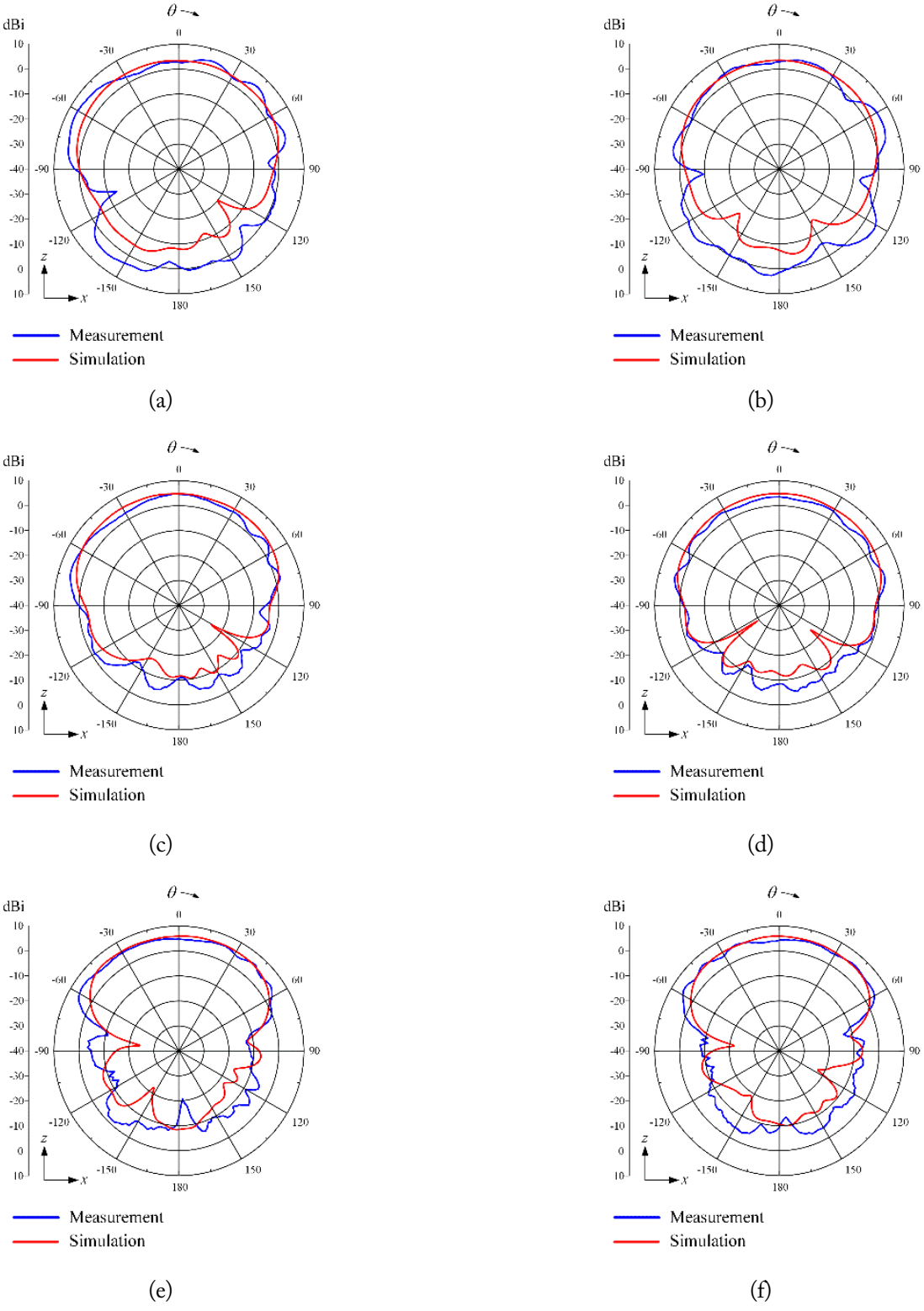

Fig. 7. Measured and simulated AEPs: (a) Ant_2 element at 2.5 GHz, (b) Ant_5 element at 2.5 GHz, (c) Ant_2 element at 3.5 GHz, (d) Ant_5 element at 3.5 GHz, (e) Ant_2 element at 4.5 GHz, and (f) Ant_5 element at 4.5 GHz.

III. Beam Synthesis using the Broadband LPDA

Beam synthesis can be conducted through the superposition of several array patterns $b_m f(\theta, \theta_m)$ with different steering angles θ_m and amplitudes b_m, as shown in a equation as follow [12]:

$$F(\theta) = b_1 f(\theta, \theta_1) + b_2 f(\theta, \theta_2) + \cdots + b_m f(\theta, \theta_m) + \cdots + b_{M-1} f(\theta, \theta_{M-1}) + b_M f(\theta, \theta_M), \quad (3)$$

Here, b_m is the required amplitude weighting, and θ_m is the steering angle for each array pattern. For example, when a guide

mask for the desired beam shape is defined in Fig. 8(a), the most appropriate beam pattern can be obtained by the superposition of multiple array patterns. Notably, to derive a synthesized beam shape that closely resembles the guided mask, a narrow HPBW and a low sidelobe level (SLL) is required for each array pattern. Therefore, the Taylor window weighting method is applied to each array pattern to achieve a low SLL using an equation as follow:

$$f(\theta,\theta_m)=\sum_{n-1}^{N} a_n g_n(\theta,\theta_m). \tag{4}$$

Here, a_n represents the weighted amplitude applied to the n^{th} element in the Taylor window, and $g_n(\theta,\theta_m)$ denotes the AEP of the n^{th} element with steering angle θ_m. The array patterns for the designed 8 × 1 array when using Taylor window weighting are shown in Fig. 8(b). The resulting measurements using AEPs exhibited an HPBW of 17.4° and an SLL of 19.4 dB.

Following this, beam synthesis for the flat-top beam, cosecant-squared beam, and iso-flux beam were carried out using Taylor window-weighted array patterns. Notably, the root-mean-square error (RMSE) lies within the range of 0 and 1, meaning that an RMSE of 0.2 indicates an error of 20%, which can be evaluated as a relatively small error. The RMSE was calculated as an evaluation metric to observe the similarity of the beam pattern shape between the measurement results and the guided mask. This can be obtained using an equation as follow:

$$\text{RMSE}=\sqrt{\frac{1}{L}\sum_{\theta=-90^\circ}^{90^\circ}(F(\theta)-G(\theta))^2}. \tag{5}$$

Here, $F(\theta)$ represents the normalized directivity of the synthesized beam, and $G(\theta)$ is the value of the guided mask at angle θ. Notably, since there are 91 sampling points (L) between −90° and 90°, the synthesized beam and the guided mask were compared by examining 91 uniformly distributed points between −90° to 90°.

Fig. 9(a) depicts the synthesized flat-top beams, which are generally used for searching and detecting targets at wide scan angles. The goals of the flat-top beam were to achieve a beamwidth of 80° (−40 ≤ θ ≤ 40° and an SLL of more than 10 dB. Beam synthesis was performed by determining the amplitude b_m when the number of array patterns M was 30. When using the measured AEPs, the results showed a beamwidth of 75° and an RMSE of 0.159 compared to the guided mask.

Fig. 9(b) illustrates the cosecant-squared beam, which is typically used for high-power airborne jamming systems. Similar to the method described previously, the cosecant-squared beam was obtained based on the guided mask ($\text{cosec}^2(11.2^\circ)$ at −40° ≤ θ ≤ −31.6° and $\text{cosec}^2(\theta+40^\circ)$ at −31.6° ≤ θ ≤ 40°), resulting in the optimum b_m (M = 30) for the most appropriate synthesized beam. The cosecant-squared beam was set to maintain a difference of 7.27 dB between the maximum and minimum values within 80° of the beamwidth. The results of the cosecant-squared beam showed that the shape attained a maximum directivity of 0 dB at θ = −30° and a reduced directivity of −7.55 dB at θ = 40°, thus achieving an RMSE of 0.167 compared to the guided mask.

Fig. 9(c) presents the results of the iso-flux beam, which is generally used in the earth-observing missions of satellites. Similar to the previous beams, the iso-flux beam was also obtained based on the guided mask ($1.5\times10^{-3}\theta^2+1$ at −40° ≤ θ ≤ 40°). Its beamwidth was set to 80° and gain difference was set to 5.4 dB. When using the measured AEPs, the iso-flux beam exhibited right-side peak directivity at θ = 32° and left-side peak at θ = −32°. In the boresight direction (θ = 0°), a low directivity of −3.57 dB was observed, and an RMSE of 0.162 was obtained compared to the guided mask.

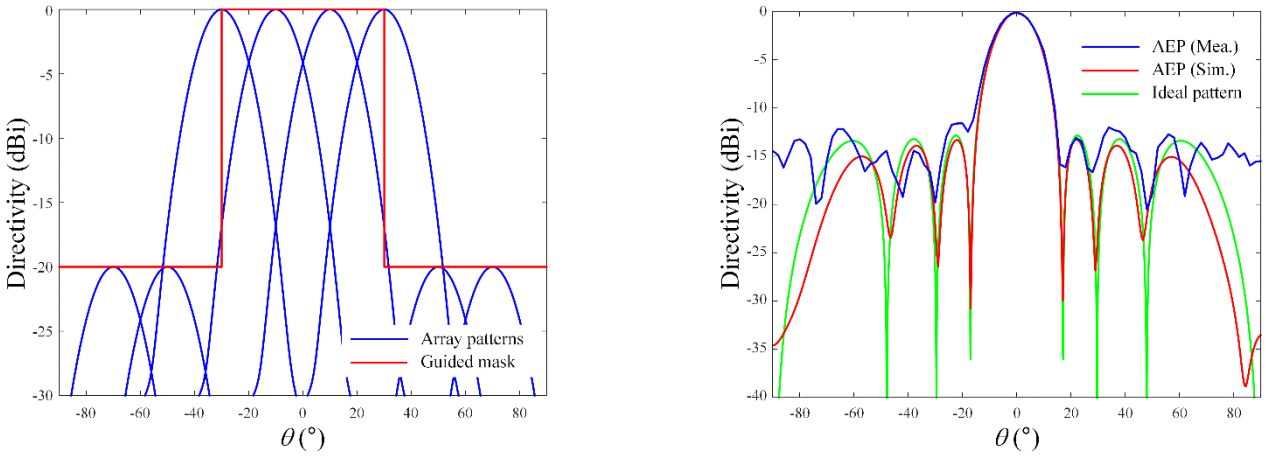

(a) (b)

Fig. 8. Beam synthesis using Taylor window-weighted array patterns: (a) superposition of array patterns for beam synthesis and (b) Taylor window-weighted array patterns.

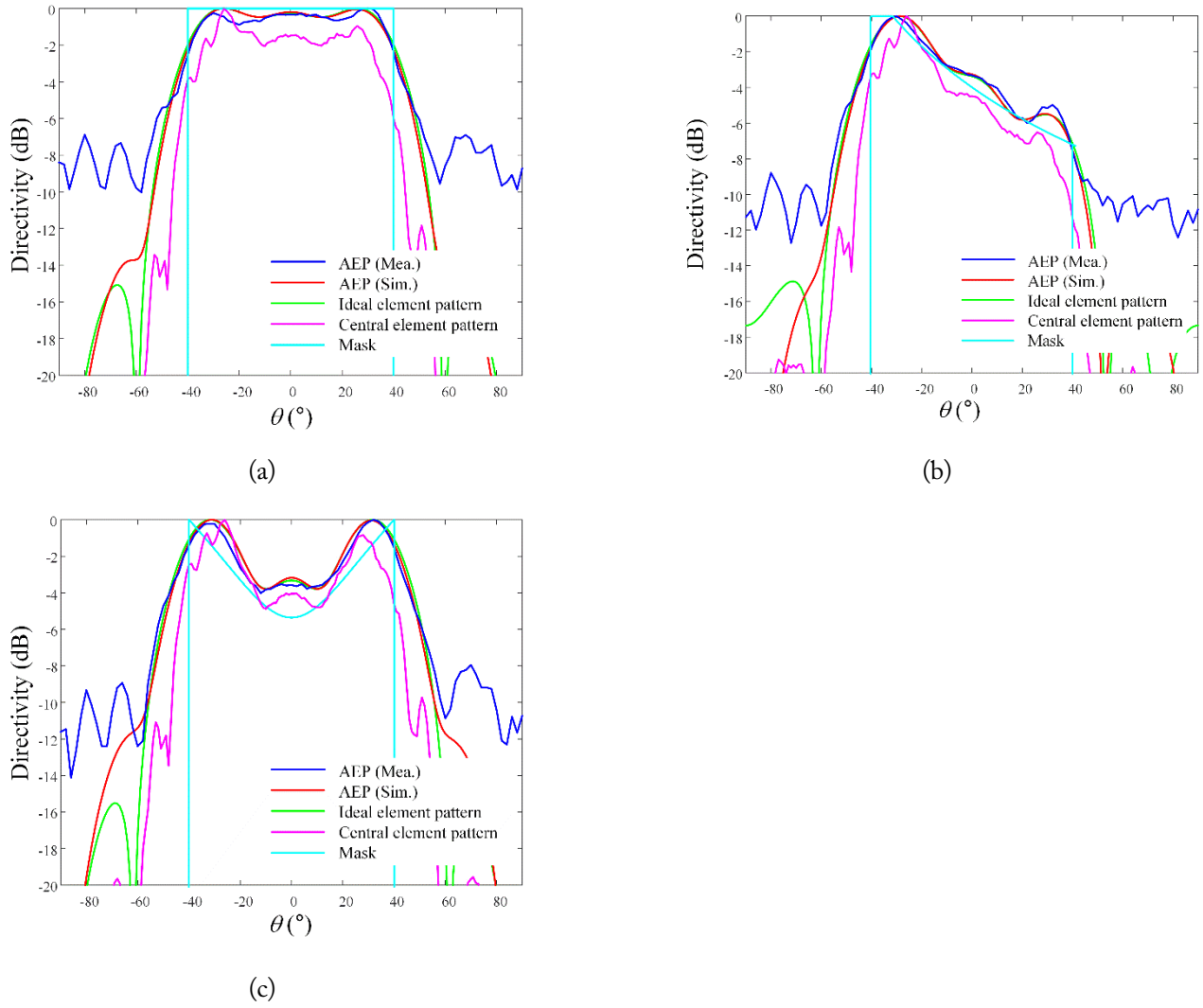

Fig. 9. Synthesized beam patterns using measured and simulated active element patterns of the designed LPDA: (a) flat-top beam pattern, (b) cosecant-squared beam pattern, and (c) iso-flux beam pattern.

This study used a different number of M based on the shape of the synthesized beam. Notably, an inadequate number of M results in multiple nulls in the synthesized beam, whereas an excessive number of M increases the SLL of the beam. Therefore, an appropriate value of M should be used to derive the beam that best resembles the shape of the mask. The results of this study confirm that various beam shapes for high-power electronic warfare applications can be achieved using the AEPs of the designed LPDA. To compare the similarities between the measurement and simulation results, the RMSEs obtained with regard to the guided masks are listed in Table 2. It is evident that the measurement results of the synthesized beams are similar to the simulation results at $-40^\circ \leq \theta \leq 40^\circ$, as indicated by the low RMSEs. However, a relatively high difference was observed in the case of SLLs. These differences may be attributed to the fact that measurement results usually show degraded performance compared to theoretical simulation results due to various reasons, such as measurement conditions, fabrication errors, and cable loss [22, 23]. In particular, since SLLs are more sensitive to errors, they exhibit greater degradation. Moreover, the performance degradation observed in the measurement can occur when the fabricated antenna is applied to the system. Therefore, when conducting beam synthesis research, it is crucial to confirm performance through fabrication.

Table 2. RMSEs of the synthesized beam patterns

Beam shape	Measurement	Simulation	Ideal pattern
Flat-top beam	0.159	0.145	0.081
Cosecant-squared beam	0.167	0.168	0.239
Iso-flux beam	0.162	0.198	0.184

IV. CONCLUSION

In this paper, various beam shapes for high-power electronic warfare applications were derived using an actual broadband

array antenna. Specifically, a compact printed LPDA with broadband characteristics was fabricated and measured for use in a limited mounting space. Subsequently, the LPDA was extended to an 8 × 1 linear array, while AEPs were obtained through measurement and simulation. The measured ARC was less than −10 dB within the 2.2–5 GHz band, while the measured boresight gains were more than 10 dBi from 2 GHz. Furthermore, beam synthesis was performed by the superposition of several array patterns with different steering angles and amplitudes. The flat-top beam achieved a beamwidth of 75° and an RMSE of 0.159. The cosecant-squared beam, which attained maximum directivity at $\theta = -30°$ and a reduced directivity of −7.55 dB at 40° achieved an RMSE of 0.167 compared to the guided mask. In addition, the iso-flux beam obtained an RMSE of 0.162 compared to the guided mask. These results were compared with those of the beam shapes obtained using ideal isotropic patterns, which ultimately confirmed that various beam shapes can be achieved in high-power electronic warfare applications using the actual array antenna.

This work was supported by the Basic Science Research Program through the National Research Foundation of Korea (NRF) funded by the Ministry of Education (No. NRF-2017R1A5A1015596), as well as by the NRF grant funded by the Korean government (No. 2015R1A6A1A03031833).

References

[1] X. Chen, T. Shu, K. B. Yu, J. He, and W. Yu, "Joint adaptive beamforming techniques for distributed array radars in multiple mainlobe and sidelobe jammings," *IEEE Antennas and Wireless Propagation Letters*, vol. 19, no. 2, pp. 248-252, 2020. https://doi.org/10.1109/LAWP.2019.2958687

[2] L. Paulsen, T. Hoffmann, C. Fulton, M. Yeary, A. Saunders, D. Thompson, B. Chen, A. Guo, and B. Murmann, "Impact: a low cost, reconfigurable, digital beamforming common module building block for next generation phased arrays," in *Proceedings of SPIE 9479: Open Architecture/Open Business Model Net-Centric Systems and Defense Transformation 2015*. Bellingham, WA: International Society for Optics and Photonics, 2015, pp. 16-30. https://doi.org/10.1117/12.2179712

[3] A. E. Spezio, "Electronic warfare systems," *IEEE Transactions on Microwave Theory and Techniques*, vol. 50, no. 3, pp. 633-644, 2002. https://doi.org/10.1109/22.989948

[4] B. Barshan and B. Eravci, "Automatic radar antenna scan type recognition in electronic warfare," *IEEE Transactions on Aerospace and Electronic Systems*, vol. 48, no. 4, pp. 2908-2931, 2012. https://doi.org/10.1109/TAES.2012.6324669

[5] N. T. Nguyen, R. Sauleau, M. Ettorre, and L. Le Coq, "Focal array fed dielectric lenses: an attractive solution for beam reconfiguration at millimeter waves," *IEEE Transactions on Antennas and Propagation*, vol. 59, no. 6, pp. 2152-2159, 2011. https://doi.org/10.1109/TAP.2011.2144550

[6] Z. Yang, Y. Chen, and S. Yang, "Scanning Radiation pattern synthesis using characteristic mode of airship platform," in *Proceedings of 2021 IEEE International Workshop on Electromagnetics: Applications and Student Innovation Competition (iWEM)*, Guangzhou, China, 2021, pp. 1-3. https://doi.org/10.1109/iWEM53379.2021.9790716

[7] S. K. Biswas and V. Chandrasekar, "Cross-validation of observations between the GPM dual-frequency precipitation radar and ground based dual-polarization radars," *Remote Sensing*, vol. 10, no. 11, article no. 1773, 2018. https://doi.org/10.3390/rs10111773

[8] I. Chiba, Y. Konishi, and T. Nishino, "Progress of phased array systems in Japan," in *Proceedings of 2010 IEEE International Symposium on Phased Array Systems and Technology*, Waltham, MA, USA, 2010, pp. 19-28. https://doi.org/10.1109/ARRAY.2010.5613395

[9] A. Rao, A. Chatterjee, J. Payne, J. Trujillo, M. Blefko, and J. Kmieciak, "Design options for a multi-beam/multi-band airborne antenna," in *Proceedings of 2019 13th European Conference on Antennas and Propagation (EuCAP)*, Krakow, Poland, 2019, pp. 1-4.

[10] Y. Aslan, J. Puskely, A. Roederer, and A. Yarovoy, "Multiple beam synthesis of passively cooled 5G planar arrays using convex optimization," *IEEE Transactions on Antennas and Propagation*, vol. 68, no. 5, pp. 3557-3566, 2020. https://doi.org/10.1109/TAP.2019.2955885

[11] J. Y. Li, Y. X. Qi, and S. G. Zhou, "Shaped beam synthesis based on superposition principle and Taylor method," *IEEE Transactions on Antennas and Propagation*, vol. 65, no. 11, pp. 6157-6160, 2017. https://doi.org/10.1109/TAP.2017.2754468

[12] H. Patidar, V. Maheshwari, R. Kar, P. K. Singh, and V. K. Sahu, "Comparative study of evolutionary algorithms to generate flat-top beam pattern for synthesis of a linear antenna array," *ICTACT Journal on Communication Technology*, vol. 12, no. 3, pp. 2519-2526, 2021.

[13] H. Patidar, G. K. Mahanti, and R. Muralidharan, "Synthesis of flat-top beam pattern of linear antenna arrays with restricted side lobe level, VSWR and independent nulls using Flower Pollination algorithm," *International Journal of Electronics*, vol. 106, no. 12, pp. 1964-1977, 2019. https://doi.org/10.1080/00207217.2019.1636297

[14] S. Dai, M. Li, Q. H. Abbasi, and M. A. Imran, "A zero placement algorithm for synthesis of flat top beam pattern with low sidelobe level," *IEEE Access*, vol. 8, pp. 225935-225944, 2020. https://doi.org/10.1109/ACCESS.2020.3045287

[15] L. F. Yepes, D. H. Covarrubias, M. A. Alonso, and R. Ferrus, "Hybrid sparse linear array synthesis applied to phased antenna arrays," *IEEE Antennas and Wireless Propagation Let-*

ters, vol. 13, pp. 185-188, 2014. https://doi.org/10.1109/LAWP.2014.2301012

[16] G. Oliveri, L. Poli, and A. Massa, "Maximum efficiency beam synthesis of radiating planar arrays for wireless power transmission," *IEEE Transactions on Antennas and Propagation*, vol. 61, no. 5, pp. 2490-2499, 2013. https://doi.org/10.1109/TAP.2013.2241714

[17] H. S. Yoon, D. G. Jo, D. I. Kim, and K. W. Choi, "On-off arbitrary beam synthesis and non-interactive beam management for phased antenna array communications," *IEEE Transactions on Vehicular Technology*, vol. 70, no. 6, pp. 5959-5973, 2021. https://doi.org/10.1109/TVT.2021.3078781

[18] J. I. Echeveste, M. A. G. de Aza, and J. Zapata, "Shaped beam synthesis of real antenna arrays via finite-element method, Floquet modal analysis, and convex programming," *IEEE Transactions on Antennas and Propagation*, vol. 64, no. 4, pp. 1279-1286, 2016. https://doi.org/10.1109/TAP.2016.2526038

[19] S. Lei, W. Yang, Z. Lin, Z. He, H. Hu, Z. Zhao, and Y. Bao, "An excitation-DRR control approach for wide-beam power gain pattern synthesis," *Signal Processing*, vol. 204, article no. 108858, 2023. https://doi.org/10.1016/j.sigpro.2022.108858

[20] Z. Lin, H. Hu, S. Lei, R. Li, J. Tian, and B. Chen, "Low-sidelobe shaped-beam pattern synthesis with amplitude constraints," *IEEE Transactions on Antennas and Propagation*, vol. 70, no. 4, pp. 2717-2731, 2022. https://doi.org/10.1109/TAP.2021.3125319

[21] R. Elliott and G. Stern, "A new technique for shaped beam synthesis of equispaced arrays," *IEEE Transactions on Antennas and Propagation*, vol. 32, no. 10, pp. 1129-1133, 1984. https://doi.org/10.1109/TAP.1984.1143216

[22] Y. M. Pan, K. W. Leung, and K. M. Luk, "of the millimeter-wave rectangular dielectric resonator antenna using a higher-order mode," *IEEE Transactions on Antennas and Propagation*, vol. 59, no. 8, pp. 2780-2788, 2011. https://doi.org/10.1109/TAP.2011.2158962

[23] S. G. Zhou, P. Dong, G. L. Huang, and J. Y. Li, "Wideband antenna array with full metal structure and air-filled microstrip feeding network," *IEEE Transactions on Antennas and Propagation*, vol. 65, no. 6, pp. 3041-3048, 2017. https://doi.org/10.1109/TAP.2017.2681319

Changhyeon Im
https://orcid.org/0000-0002-8973-4398

received his B.S. degree in electronic and electrical engineering from Hongik University, Seoul, South Korea, in 2021, where he is currently pursuing his Ph.D. in electronic and electrical engineering. His research interests include mesh reflector antennas, 5G applications, wireless power transfer, and ultra-wideband antennas.

Sangwoon Youn
https://orcid.org/0000-0003-1437-8445

received his B.S. and M.S. degrees in electronic and electrical engineering from Hongik University, Seoul, South Korea, in 2019 and 2021, respectively, where he is currently pursuing a Ph.D. in electronic and electrical engineering. His research interests include EMI and EMC, wave propagation, UWB antennas, 5G applications, and direction-finding and anti-jamming systems.

Tae Heung Lim
https://orcid.org/0000-0001-7968-1272

received the B.S., M.S., and Ph.D degrees in electronic and electrical engineering from Hongik University, Seoul, South Korea, in 2016, 2018, and 2022, respectively. He was a Postdoctoral Researcher in Ulsan National Institute of Science and Technology (UNIST) in 2022. He was a Senior Researcher with the Agency for Defense Development, Daejon, South Korea in 2023. He is currently an assistant professor with the School of Electronic Engineering, Kumoh National Institute of Technology. His research interests include space surveillance radar, 6G system antennas, sea-based radar, high-power array antennas, adaptive beamforming, and wave propagations for radar applications.

Hosung Choo
https://orcid.org/0000-0002-8409-6964

received his B.S. degree in radio science and engineering from Hanyang University, Seoul, South Korea, in 1998, and his M.S. and Ph.D. degrees in electrical and computer engineering from the University of Texas at Austin in 2000 and 2003, respectively. In September 2003, he joined the School of Electronic and Electrical Engineering, Hongik University, Seoul, where he is currently a professor. His principal areas of research include electrically small antennas for wireless communications, reader and tag antennas for RFID, on-glass and conformal antennas for vehicles and aircrafts, and array antennas for GPS applications.